TEST VALIDATION OF EXTENSION-TWISTING COUPLED LAMINATES WITH MATCHED ORTHOTROPIC STIFFNESS.

Christopher B. York[1] and Kim Kheng Lee[2]

[1]Singapore Institute of Technology, Dover Drive, Singapore 138683

[2]Singapore Polytechnic, 500 Dover Road, Singapore 139651

Abstract

An experimental validation study is presented for three classes of coupled laminate with matching *Extension-Twisting* coupling. The designs also have matching orthotropic stiffness, in both extension and bending, and have been chosen specifically to investigate the influence of mechanical *Extension-Shearing* and/or *Bending-Twisting* on the performance of *Extension-Twisting* coupled designs under axial tension loads. All designs are Hygro-Thermally Curvature Stable (HTCS) or warp-free.

Keywords

Extension-Twisting coupling; Hygro-thermally Curvature Stable; *Extension-Shearing* coupling; *Bending-Twisting coupling*; Laminate Stacking Sequences.

Nomenclature

$\mathbf{A}$,A_{ij}	=	extensional (membrane) stiffness matrix and its elements (i,j = 1, 2, 6), N/mm.
$\mathbf{a}$,a_{ij}	=	extensional (membrane) compliance matrix and its elements (i,j = 1, 2, 6), $(N/mm)^{-1}$.
$\mathbf{B}$,B_{ij}	=	bending-extension-coupling stiffness matrix and its elements (i,j = 1, 2, 6), N.
$\mathbf{b}$,b_{ij}	=	bending-extension-coupling compliance matrix and its elements (i,j = 1, 2, 6), $(N)^{-1}$.
$\mathbf{D}$,D_{ij}	=	bending (flexural) stiffness matrix and its elements (i,j = 1, 2, 6), N.mm.
$\mathbf{d}$,d_{ij}	=	bending (flexural) compliance matrix and its elements (i,j = 1, 2, 6), $(N.mm)^{-1}$.
H	=	laminate thickness (= $n \times t$), mm
n	=	number of plies in laminate stacking sequence.
$\mathbf{N}$	=	in-plane force resultants (= $\{N_x, N_y, N_{xy}\}^T$), N/mm.
N_x,N_y	=	in-plane axial load per unit length, N/mm.
N_{xy}	=	in-plane shear flow, N/mm.
$\mathbf{M}$	=	moment resultants (= $\{M_x, M_y, M_{xy}\}^T$), N.mm/mm.
M_x,M_y	=	bending moments per unit length about principal axes, N.mm/mm.
M_{xy}	=	twist moment per unit length, N.mm/mm.
Q_{ij}	=	reduced stiffness (i,j = 1, 2, 6), N/mm^2.

Q'_{ij} = transformed reduced stiffness (i,j = 1, 2, 6), N/mm^2.

t = ply thickness, mm.

U_i = laminate invariant properties (i = 1 - 5), N/mm^2.

x,y,z = principal axes.

β = offset angle between principal axes and material axes, deg.

$\boldsymbol{\varepsilon}$ = in-plane strains (= $\{\varepsilon_x, \varepsilon_y, \gamma_{xy}\}^T$), mm/mm.

$\varepsilon_x, \varepsilon_y$ = in-plane axial strains, mm/mm.

γ_{xy} = in-plane shear strain, rad.

$\boldsymbol{\kappa}$ = curvatures (= $\{\kappa_x, \kappa_y, \kappa_{xy}\}^T$), mm^{-1}.

κ_x, κ_y = curvatures about principal axes, mm^{-1}.

κ_{xy} = twist curvature, mm^{-1}.

$\xi_{1\text{-}4}$ = lamination parameters for extensional stiffness.

$\xi_{5\text{-}8}$ = lamination parameters for coupling stiffness.

$\xi_{9\text{-}12}$ = lamination parameters for bending stiffness.

1. Introduction

This article focuses on the experimental validation of recently identified laminates [1-3] possessing Hygro-Thermally Curvature-Stable or HTCS properties [4-8]. The identification of stacking sequence configurations which satisfy the HTCS condition allows a broad range of complex mechanical

coupling attributes to be exploited without the complicating issue of thermal distortions, which are a consequence of the high temperature curing process.

Relatively few articles [8] have considered properties beyond isolated *Extension-Twisting* coupling, although it should be noted that *Extension-Twisting* coupled designs also possess an inseparable *Shearing-Bending* coupling counterpart, but this is not active under axial tension loading.

Coupled laminates are described here in terms of their response to various combinations of force and moment resultants, from either mechanical, thermal and/or moisture effects, using a cause and effect relationship. A laminate is therefore described as an *E-S* laminate if extension (*E*) causes a shearing (*S*) effect and is said to possess *Extension-Shearing* coupling. If bending (*B*) causes a twisting (*T*) effect, the laminate is described as a *B-T* laminate and is said to possess *Bending-Twisting* coupling. The four characters *E*, *S*, *B*, and *T* can be used in any combination to describe cause and effect relationship in all coupled laminates [1]; noting that each cause and effect pair is reversible.

Stacking sequence configurations for HTCS laminates have been identified [2] in nine of twenty-four classes of coupled laminate with standard ply angle orientations ±45, 0 and 90°. All arise from the judicious re-alignment of the principal material axis of laminates possessing *Bending-Extension* and *Twisting-Shearing* or *B-E-T-S* coupling, or additionally possessing *Bending-Twisting*, i.e., *B-E-T-S*;*B-T* coupling. The off-axis alignments of these two parent classes then give rise to the other more complex combinations, which include: *Extension-Shearing* or *E-S* coupling; *Bending-Extension* and *Twisting-Shearing* or *B-E-T-S* coupling or; *Extension-Bending*, *Shearing-Bending*, *Extension-Twisting* and *Shearing-Twisting* or *E-B-S-B-E-T-S-T*.

The challenge here is to identify whether any of these complex mechanical coupling properties are of practical significance. Certainly, in recent years, there has been a significant increase in the use of solid rotor blades, which have so far been associated with unmanned air vehicles, but are now finding

application in manned air vehicles, such as the Volocopter; a multicopter, adopting an array of 18 rotor blades. *Extension-Twisting* coupled blades have the potential to augment lift characteristics through a change in rotor speed, and the resulting extensional (centrifugal) forces. However, the design of such aero-elastic compliant rotor blades with tailored *Extension-Twisting* coupling properties, is an example of a laminate design that, from a manufacturing perspective, requires either specially curved tooling or HTCS properties in order to remain flat after high temperature curing. Therefore, new families of HTCS laminates, with complex mechanical coupling behaviour, are now investigated to assess the performance benefits, such as twist augmentation, from interactions between *Extension*, *Shearing*, *Bending* and *Twisting* on otherwise identical *Extension-Twisting* coupled designs.

The necessary conditions for HTCS laminates are presented, after a summary of the basic relationships between the ABD matrix of stiffness components and lamination parameters, which are adopted here to simplify the mechanical and thermal characterization. An overview of the database of stacking sequence configurations [2], developed subsequently, is also given.

Stacking sequence configurations within the database are then filtered for matching orthotropic stiffness in extension and bending, as well as coupling behaviour, to reveal designs with additional coupling responses, specifically mechanical *Extension-Shearing* and/or *Bending-Twisting*. The effect of these additional couplings, and how they influence the performance of *Extension-Twisting* coupled designs under axial tension loads is then assessed experimentally, for validation of numerical predictions.

The following section provides the basic relationships between the ABD relation and lamination parameters, which helps to simplify the mechanical and thermal characterization.

2. Relationship between Lamination Parameters and Laminate Stiffnesses.

Lamination parameters provide a convenient way of matching ply angle dependent properties within the database of stacking sequences [2] for a defined number of plies, n, of constant thickness, t, or overall thickness H (= $n \times t$). Elements of the extensional [A], coupling [B] and bending [D] stiffness matrices are related to the lamination parameters and laminate invariants, respectively, by:

$$A_{11} = \{U_1 + \xi_1 U_2 + \xi_2 U_3\} \times H \tag{1}$$

$$A_{12} = A_{21} = \{-\xi_2 U_3 + U_4\} \times H$$

$$A_{16} = A_{61} = \{\xi_3 U_2/2 + \xi_4 U_3\} \times H$$

$$A_{22} = \{U_1 - \xi_1 U_2 + \xi_2 U_3\} \times H$$

$$A_{26} = A_{62} = \{\xi_3 U_2/2 - \xi_4 U_3\} \times H$$

$$A_{66} = \{-\xi_2 U_3 + U_5\} \times H$$

$$B_{11} = \{\xi_5 U_2 + \xi_6 U_3\} \times H^2/4 \tag{2}$$

$$B_{12} = B_{21} = \{-\xi_6 U_3\} \times H^2/4$$

$$B_{16} = B_{61} = \{\xi_7 U_2/2 + \xi_8 U_3\} \times H^2/4$$

$$B_{22} = \{-\xi_5 U_2 + \xi_6 U_3\} \times H^2/4$$

$$B_{26} = B_{62} = \{\xi_7 U_2/2 - \xi_8 U_3\} \times H^2/4$$

$$B_{66} = \{-\xi_6 U_3\} \times H^2/4$$

$$D_{11} = \{U_1 + \xi_9 U_2 + \xi_{10} U_3\} \times H^3/12 \quad (3)$$

$$D_{12} = D_{21} = \{-\xi_{10} U_3 + U_4\} \times H^3/12$$

$$D_{16} = D_{61} = \{\xi_{11} U_2/2 + \xi_{12} U_3\} \times H^3/12$$

$$D_{22} = \{U_1 - \xi_9 U_2 + \xi_{10} U_3\} \times H^3/12$$

$$D_{26} = D_{62} = \{\xi_{11} U_2/2 - \xi_{12} U_3\} \times H^3/12$$

$$D_{66} = \{-\xi_{10} U_3 + U_5\} \times H^3/12$$

where the laminate invariants are calculated from the reduced stiffness terms, Q_{ij}:

$$U_1 = \{3Q_{11} + 3Q_{22} + 2Q_{12} + 4Q_{66}\}/8 \quad (4)$$

$$U_2 = \{Q_{11} - Q_{22}\}/2$$

$$U_3 = \{Q_{11} + Q_{22} - 2Q_{12} - 4Q_{66}\}/8$$

$$U_4 = \{Q_{11} + Q_{22} + 6Q_{12} - 4Q_{66}\}/8$$

$$U_5 = \{Q_{11} + Q_{22} - 2Q_{12} + 4Q_{66}\}/8$$

and the reduced stiffness terms are calculated from the engineering constants of the ply material:

$$Q_{11} = E_1/(1 - \nu_{12}\nu_{21}) \quad (5)$$

$$Q_{12} = \nu_{12} E_2/(1 - \nu_{12}\nu_{21})$$

$$Q_{22} = E_2/(1 - \nu_{12}\nu_{21})$$

$$Q_{66} = G_{12}$$

3. Hygro-Thermally Curvature-Stable or Warp-Free laminates

The manufacture of any general *Extension-Twisting* coupled laminate presents a particular challenge if such mechanical coupling behaviour is required without the thermal distortions that arise as a consequence of the high temperature curing process. In such cases, the HTCS or thermally warp-free condition offers a manufacturing solution, but with an inevitable restriction in the magnitude of the mechanical coupling.

For extensionally isotropic laminates with standard ply orientations ±45, 0 and 90°, lamination parameters or the equivalent extensional and coupling stiffness elements must satisfy the requirements of Table 1. For square symmetric in-plane properties, in which the fully isotropic properties are not satisfied the constraints on HTCS laminates may be relaxed in comparison to those stated in Table 1, i.e.: $\xi_1 = \xi_3 = 0$.

These conditions correspond to extensional stiffnesses of the following form:

$$\begin{bmatrix} A_{11} & A_{12} & A_{16} \\ A_{12} & A_{11} & -A_{16} \\ A_{16} & -A_{16} & A_{66} \end{bmatrix} \tag{6}$$

which represent the square symmetric form of the extensional stiffness matrix for off-axis material alignment. For coincident material and structural axis alignment, the constraints include $\xi_4 = 0$, which correspond to extensional stiffnesses of the following form:

$$\begin{bmatrix} A_{11} & A_{12} & 0 \\ A_{12} & A_{11} & 0 \\ 0 & 0 & A_{66} \end{bmatrix} \tag{7}$$

Note that the HTCS conditions are independent of the nature of the bending stiffness.

The database of laminate designs [2] contains definitive listings of all forms of coupled HTCS laminate. These are presented in symbolic form, together with non-dimensional parameters; making each configuration independent of both material properties and fibre orientations. Fibre directions are required to have a specific angle separation to achieve HTCS properties and whilst commonly adopted angles are used here, i.e., 0, ±45 and 90°, other angle separations have been shown to be possible [9].

The choice of 16 ply laminates for the experimental test allows a rich design space for stiffness matching, since the design space representing *E-B-S-T;B-T* coupled extensionally isotropic laminates contains 6, 280, 23,652 and 2,379,722 sequences with 8, 12, 16 and 20 plies, respectively. Whilst extensional isotropy is retained, *Bending-Twisting* coupling is present for all off-axis alignments. However, there are a number of exceptions: 3, 10 and 126 cases arise for 8-, 12- and 16-ply laminates for which off-axis alignment $\beta = \pi/8 + m\pi/2$ ($m = 0, 1, 2, 3$), renders the laminate uncoupled in bending, i.e. $D_{16} = D_{26} = 0$. This gives rise to the *E-T-S-B* coupling properties of interest. It was from this relatively small group of designs that Laminate 1 of Table 2 was chosen.

The choice of the comparator designs was then sought with matching orthotropic extensional and bending stiffness as well as coupling stiffness properties.

The design space representing *E-B-S-T* coupled laminates with extensional isotropy, contains 8, 264 and 17,118 sequences with 12, 16 and 20 plies, respectively, but apart from 8 quasi-homogeneous solutions, where $D_{ij} = A_{ij}H^2/12$, all develop *Bending-Twisting* coupling for any off-axis material alignment. The gives rise to the *E-T-S-B;B-T* coupling properties of interest, which is represented by Laminate 2 of Table 2.

The design space representing *E-B-S-T* coupled laminates with extensional square symmetry contains 6, 524, and 35,610 with 12, 16 and 20 plies, respectively, and therefore gives rise to *Extension-Shearing* as well as *Bending-Twisting* coupling for any off-axis material alignment. This provides the

E-S;E-T-S-B;B-T laminate characteristics of interest, represented by Laminate 3 of Table 2. Unfortunately, there are no 16 ply laminates for which the *Bending-Twisting* properties, D_{16} and D_{26}, could be matched precisely with Laminate 2.

4. Constitutive Relations

The constitutive relations are useful for confirming the precisely matched orthotropic and coupling stiffnesses properties across the three designs, but also for gaining a qualitative insight into the relative twist from additional coupling terms.

Engineering constants of the ply material represent carbon fibre/Epoxy (T700HS/SE 84LV) and were taken from published data, i.e., $E_1 = 131$ GPa, $E_2 = 8.2$ GPa, $G_{12} = 4.3$ GPa and $\nu_{12} = 0.38$. The lamina thickness $t = 0.163$mm, giving a 16-ply laminate thickness $H = 2.608$mm.

Laminate 1.

The ABD matrix for Laminate 1, with axis aligned properties, is given in Eqn. (8), and represents *E-B-S-T;B-T* coupling. By inspection, $A_{11} = A_{22}$, and by calculation, $A_{66} = (A_{11} - A_{12})/2 = 49{,}350$ N/mm, revealing that the laminate possesses in-plane isotropic properties.

$$\begin{Bmatrix} N_x \\ N_y \\ N_{xy} \\ \hdashline M_x \\ M_y \\ M_{xy} \end{Bmatrix} = \left[\begin{array}{ccc:ccc} 145,037 & 46,336 & 0 & 18,648 & -18,648 & 0 \\ 46,336 & 145,037 & 0 & -18,648 & 18,648 & 0 \\ 0 & 0 & 49,350 & 0 & 0 & -18,648 \\ \hdashline 18,648 & -18,648 & 0 & 97,234 & 26,264 & -7,513 \\ -18,648 & 18,648 & 0 & 26,264 & 67,181 & -7,513 \\ 0 & 0 & -18,648 & -7,513 & -7,513 & 27,972 \end{array}\right] \begin{Bmatrix} \varepsilon_x \\ \varepsilon_y \\ \gamma_{xy} \\ \hdashline \kappa_x \\ \kappa_y \\ \kappa_{xy} \end{Bmatrix} \tag{8}$$

The ABD matrix for off-axis alignment, $\beta = \pi/8$, is given in Eqn. (9), and represents *E-T-S-B* coupling with isotropic extension stiffness properties. The transformed square symmetric relationships for B_{ij}, described in Table 1, are also demonstrated.

$$\begin{Bmatrix} N_x \\ N_y \\ N_{xy} \\ \hdashline M_x \\ M_y \\ M_{xy} \end{Bmatrix} = \left[\begin{array}{ccc:ccc} 145,037 & 46,336 & 0 & 0 & 0 & 18,648 \\ 46,336 & 145,037 & 0 & 0 & 0 & -18,648 \\ 0 & 0 & 49,350 & 18,648 & -18,648 & 0 \\ \hdashline 0 & 0 & 18,648 & 103,458 & 26,264 & 0 \\ 0 & 0 & -18,648 & 26,264 & 60,957 & 0 \\ 18,648 & -18,648 & 0 & 0 & 0 & 27,972 \end{array}\right] \cdot \begin{Bmatrix} \varepsilon_x \\ \varepsilon_y \\ \gamma_{xy} \\ \hdashline \kappa_x \\ \kappa_y \\ \kappa_{xy} \end{Bmatrix} \tag{9}$$

The compliance relationship of Eqn. (10), corresponding to the inverse of Eqn. (9), reveals that a twist curvature, κ_{xy} = -0.00188/mm, arises from using a tensile load N_x = 208.3 N/mm, equivalent to a 5 kN test load.

$$10^{-6}\begin{Bmatrix} 1,955 \\ -866 \\ 0 \\ \hdashline 0 \\ 0 \\ -1,881 \end{Bmatrix} = 10^{-9}\left[\begin{array}{ccc:ccc} 9,385 & -4,159 & 0 & 0 & 0 & -9,029 \\ -4,159 & 9,385 & 0 & 0 & 0 & 9,029 \\ 0 & 0 & 27,841 & -8,062 & 11,991 & 0 \\ \hdashline 0 & 0 & -8,062 & 13,188 & -8,148 & 0 \\ 0 & 0 & 11,991 & -8,148 & 23,584 & 0 \\ -9,029 & 9,029 & 0 & 0 & 0 & 47,790 \end{array}\right]\begin{Bmatrix} 208.3 \\ 0 \\ 0 \\ \hdashline 0 \\ 0 \\ 0 \end{Bmatrix} \tag{10}$$

Laminate 2.

The ABD matrix for Laminate 2, with axis aligned properties representing *E-B-S-T* coupling, is given in Eqn (11). Once again, the extensional stiffness properties are isotropic.

$$\begin{Bmatrix} N_x \\ N_y \\ N_{xy} \\ \hdashline M_x \\ M_y \\ M_{xy} \end{Bmatrix} = \left[\begin{array}{ccc:ccc} 145,037 & 46,336 & 0 & 18,648 & -18,648 & 0 \\ 46,336 & 145,037 & 0 & -18,648 & 18,648 & 0 \\ 0 & 0 & 49,350 & 0 & 0 & -18,648 \\ \hdashline 18,648 & -18,648 & 0 & 117,327 & 21,198 & 0 \\ -18,648 & 18,648 & 0 & 21,198 & 57,220 & 0 \\ 0 & 0 & -18,648 & 0 & 0 & 22,906 \end{array}\right]\begin{Bmatrix} \varepsilon_x \\ \varepsilon_y \\ \gamma_{xy} \\ \hdashline \kappa_x \\ \kappa_y \\ \kappa_{xy} \end{Bmatrix} \tag{11}$$

The ABD matrix for off-axis alignment, $\beta = \pi/8$, is given in Eqn. (12), and represents *E-T-S-B;B-T* coupling with precisely matching stiffness properties to those of Laminate 1, with the exception that *Bending-Twisting* coupling terms, D_{16} and D_{26} are now introduced.

$$\begin{Bmatrix} N_x \\ N_y \\ N_{xy} \\ \hline M_x \\ M_y \\ M_{xy} \end{Bmatrix} = \left[\begin{array}{ccc:ccc} 145,037 & 46,336 & 0 & 0 & 0 & 18,648 \\ 46,336 & 145,037 & 0 & 0 & 0 & -18,648 \\ 0 & 0 & 49,350 & 18,648 & -18,648 & 0 \\ \hdashline 0 & 0 & 18,648 & 103,458 & 26,264 & 15,692 \\ 0 & 0 & -18,648 & 26,264 & 60,957 & 5,559 \\ 18,648 & -18,648 & 0 & 15,692 & 5,559 & 27,972 \end{array}\right] \begin{Bmatrix} \varepsilon_x \\ \varepsilon_y \\ \gamma_{xy} \\ \hline \kappa_x \\ \kappa_y \\ \kappa_{xy} \end{Bmatrix} \tag{12}$$

The compliance matrix of Eqn (13) is fully populated as a result of the *Bending-Twisting* coupling terms, D_{16} and D_{26}, which is discussed in more detail at the end of this section. However, for the unconstrained case, represented by the constitutive relations, only the b_{16} term influences the magnitude of the twist curvature, κ_{xy} = -0.00214/mm, which corresponds to a twist augmentation of 14% above Laminate 1.

$$10^{-6}\begin{Bmatrix} 2,005 \\ -916 \\ -128 \\ 346 \\ 7 \\ -2,143 \end{Bmatrix} = 10^{-9}\left[\begin{array}{ccc:ccc} 9,622 & -4,396 & -616 & 1,662 & 33 & -10,285 \\ -4,396 & 9,622 & 616 & -1,662 & -33 & 10,285 \\ -616 & 616 & 28,036 & -8,589 & 11,981 & 3,258 \\ \hdashline 1,662 & -1,662 & -8,589 & 14,610 & -8,120 & -8,798 \\ 33 & -33 & 11,981 & -8,120 & 23,585 & -177 \\ -10,285 & 10,285 & 3,258 & -8,798 & -177 & 54,434 \end{array}\right] \begin{Bmatrix} 208.3 \\ 0 \\ 0 \\ \hdashline 0 \\ 0 \\ 0 \end{Bmatrix} \tag{13}$$

Laminate 3.

The ABD matrix for Laminate 3, with axis aligned properties representing <u>*E-B*-*S-T;B-T*</u> coupling, is given in Eqn (14). In this case, whilst simple inspection reveals $A_{11} = A_{22}$, calculation of $A_{66} \neq (A_{11} - A_{12})/2$ = 49,350 N/mm, reveals that in-plane properties are square symmetric, and not isotropic.

$$\begin{Bmatrix} N_x \\ N_y \\ N_{xy} \\ \hline M_x \\ M_y \\ M_{xy} \end{Bmatrix} = \left[\begin{array}{ccc:ccc} 164,105 & 27,269 & 0 & 18,648 & -18,648 & 0 \\ 27,269 & 164,105 & 0 & -18,648 & 18,648 & 0 \\ 0 & 0 & 30,282 & 0 & 0 & -18,648 \\ \hdashline 18,648 & -18,648 & 0 & 113,890 & 23,562 & -537 \\ -18,648 & 18,648 & 0 & 23,562 & 55,930 & -537 \\ 0 & 0 & -18,648 & -537 & -537 & 25,270 \end{array}\right] \begin{Bmatrix} \varepsilon_x \\ \varepsilon_y \\ \gamma_{xy} \\ \hline \kappa_x \\ \kappa_y \\ \kappa_{xy} \end{Bmatrix} \tag{14}$$

The ABD matrix for off-axis alignment, $\beta = \pi/8$, is given in Eqn. (15), and represents *E-S;E-T-S-B;B-T* coupling, with precisely matching stiffness properties to those of Laminate 1, except that *Extension-Shearing* terms, A_{16} and A_{26}, as well as *Bending-Twisting* coupling terms, D_{16} and D_{26} are now introduced. Note that the square symmetric extensional stiffness properties have been transformed into equivalent isotropic properties, which occurs only at $\beta = \pi/8 + i\pi/4$, with i = 0, 1, 2, 3...., and is coincident with the maximum absolute values of A_{16} and A_{26}.

$$\begin{Bmatrix} N_x \\ N_y \\ N_{xy} \\ \hdashline M_x \\ M_y \\ M_{xy} \end{Bmatrix} = \left[\begin{array}{ccc:ccc} 145,037 & 46,336 & 19,068 & 0 & 0 & 18,648 \\ 46,336 & 145,037 & -19,068 & 0 & 0 & -18,648 \\ 19,068 & -19,068 & 49,350 & 18,648 & -18,648 & 0 \\ \hdashline 0 & 0 & 18,648 & 103,458 & 26,264 & 12,568 \\ 0 & 0 & -18,648 & 26,264 & 60,957 & 7,165 \\ 18,648 & -18,648 & 0 & 12,568 & 7,165 & 27,972 \end{array}\right] \begin{Bmatrix} \varepsilon_x \\ \varepsilon_y \\ \gamma_{xy} \\ \hdashline \kappa_x \\ \kappa_y \\ \kappa_{xy} \end{Bmatrix} \tag{15}$$

The compliance matrix of Eqn (16) is fully populated as a result of both the *Extension-Shearing* terms, A_{16} and A_{26}, and the *Bending-Twisting* coupling terms, D_{16} and D_{26}. However, for the unconstrained case, only the b_{16} term once again influences the magnitude of the twist curvature, κ_{xy} = -0.00295/mm, which corresponds to an augmentation in the twist curvature of 57% above Laminate 1.

$$10^{-6}\begin{Bmatrix} 2,586 \\ -1,498 \\ -2,214 \\ 946 \\ -737 \\ -2,959 \end{Bmatrix} = 10^{-9}\left[\begin{array}{ccc:ccc} 12,415 & -7,190 & -10,627 & 4,539 & -3,537 & -14,204 \\ -7,190 & 12,415 & 10,627 & -4,539 & 3,537 & 14,204 \\ -10,627 & 10,627 & 39,371 & -13,046 & 15,787 & 15,988 \\ \hdashline 4,539 & -4,539 & -13,046 & 15,730 & -9,513 & -10,683 \\ -3,537 & 3,537 & 15,787 & -9,513 & 25,030 & 2,580 \\ -14,204 & 14,204 & 15,988 & -10,683 & 2,580 & 58,828 \end{array}\right] \begin{Bmatrix} 208.3 \\ 0 \\ 0 \\ \hdashline 0 \\ 0 \\ 0 \end{Bmatrix} \tag{16}$$

The compliance relationships of Eqns (10), (13) and (16) reveal the complexity of the coupling interaction that is not seen in the equivalent stiffness relationships of Eqns (9), (12) and (15). Whilst the matrix of in-plane compliances, **a**, remains square symmetric, as described in Eqns (6) and (7), the matrix of coupling compliances, $\mathbf{b}^T$, does not, but instead possesses a special form, relating the first

two columns as follows: $b_{21} = -b_{11}$, $b_{12} = -b_{22}$ and/or $b_{16} = -b_{26}$. For thermal loading only, in-plane shear strain $\gamma_{xy} = 0$ and curvatures $\kappa_x = \kappa_y = \kappa_{xy} = 0$ given that thermal force resultants $N_x^{Thermal} = N_y^{Thermal}$ and $N_{xy}^{Thermal} = 0$ and the thermal moment resultants $M_x^{Thermal} = M_y^{Thermal} = M_{xy}^{Thermal} = 0$. Hence, square symmetry in **A**, **B** and **N**, with **M** = **0**, are the necessary conditions for HTCS laminates [2].

Laminates with isolated Extension-Shearing coupling and isolated *Bending-Twisting* coupling represent two of the 24 classes of mechanically coupled laminate, representing all possible interactions through the stiffness matrix representation of *Extension*, *Shearing*, *Bending* and *Twisting* [1]. When these isolated couplings are combined with *Extension-Twisting*, *Bending-Shearing* coupling, these interactions become more complex; noting that the inseparable *Bending-Shearing* coupling is not active under tensile loading. However, the compliance matrix representation of Laminate 2 demonstrates that *Extension-Shearing* behaviour is now developed because $a_{16}, a_{26} \neq 0$. Hence the addition of *Bending-Twisting* coupling stiffnesses D_{16} and D_{26} in Laminate 2 causes *Bending* because of *Twisting*, and hence *Shearing* through the inseparable but now active *Bending-Shearing* coupling.

This can be thought of as a secondary coupling and indeed the resulting shear strains under axial tension are small in comparison to Laminate 3, which possesses Extension Shearing coupling stiffnesses A_{16} and A_{26}. For the uni-axial mechanical loading applied here, shear strains $\gamma_{xy} = -128$ μ rad (-0.007°) arise for Laminate 2 and $\gamma_{xy} = -2{,}214$ μ rad (-0.127°) for Laminate 3. Nevertheless, these strain predictions are constrained, in both cases, by the mechanical grips used in the experimental tests. Similarly, curvature κ_x is inhibited under tension loading.

Compliances have been used by others [8] to investigate similar coupling effects, but this is only possible through an optimization technique, from which a set of free form angles must be developed that satisfy a set of compliance constraints. However, these techniques invariably lead to non-zero

residual terms, which are amplified when presented as a stiffness matrix representation of the stacking sequence. Additionally, stacking sequences with free form angles generally have limited practical application since they can certainly never be tapered, by applying ply drops, without destroying the desired thermo-mechanical response. By contrast the designs used in this article are taken from databases of laminate stacking sequences that can be tapered whilst maintaining both their hygro-thermal and mechanical coupling properties [9].

It was not thought possible that zero *Extension-Shearing* coupled compliances, a_{16} and a_{26}, could be achieved in the presence of *Bending-Twisting* coupled stiffnesses, when matching both *Extension-Twisting* (and inseparable *Shearing-Bending*) coupled stiffnesses as well as orthotropic *Extensional* and *Bending* stiffnesses. However, this was due to an oversight whilst interrogating the laminate databases. These designs have therefore been provided in the electronic annex to this article, since they do not affect any of the conclusions drawn here.

5. Experimental Test

Each of the three classes of coupled laminate highlighted in Table 2 were manufactured with standard fibre alignments (0, ±45, 90°) and constant thickness Carbon fibre/Epoxy (T700HS/SE 84LV) pre-preg material using a standard autoclave curing process. Specimens were then prepared at an off-axis orientation ($\beta = \pi/8$) to the manufacturing axis to induce the desired *Extension-Twisting* coupling behaviour. Thermally curvature stable predictions were validated using plates, from which test specimens were later cut, since any imperfections are amplified against precision flat surface.

Experimental validation of *Extension-Twisting* coupling behaviour was performed using an MTS BIONIX 25 kN axial-torsional servo-hydraulic test machine, see Fig. 1. The hydraulic grips were set to 6.2 MPa (900 psi) to prevent slippage of the specimens and a 0.5 mm/min extension rate was used to introduce quasi-static loading. The top hydraulic grip was actively controlled to ensure a zero-

torque condition on the specimen and the twist rotation recorded under increasing axial tension up to a maximum axial load of 5 kN (equating to N_x = 208.3 N/mm), at which the average axial displacements of 0.73mm, 0.74mm and 0.83mm were recorded for Laminates 1, 2 and 3 respectively. The specimens, waterjet cut from a plate specimen into strips, measured 240mm in length and 24mm in width, to match the dimensional constraint of the hydraulic grips. There were some width variations due to cutting inaccuracies and cured laminate thicknesses also varied across the range of specimens, with an overall thickness ranging between H = 2.53 – 2.66mm, equivalent to ply thickness t = 0.158mm – 0.166mm. Data for each specimen is presented in Table A1 of the electronic annex. The gauge length was 189 mm and confirmed after testing from indentations on the specimens by the bevelled edge grips, see Fig. A1 of the electronic annex.

6. Finite element modelling

An Abaqus non-linear Finite Element (Riks) analysis was used [10] to predict the *Extension-Twisting* coupling response for comparison with the experimental tests using 4-noded shell elements (S4R). A converged solution was obtained with 1mm square elements. One end of the model was constrained to simulate the fully-clamped condition, whilst at the other edge, extension was permitted only in the loading axis direction together with rotational freedom around the same axis. These boundary conditions were found necessary for Laminate 3 to enforce *Extension-Twisting* without *Extension-Bending* and *Extension-Shearing* coupling. This secondary coupling behaviour is illustrated in Fig. 3, where the reference node, denoted by a cross on the views along the centre line or loading axis of the specimen, migrates from loading axis during the *Extension-Twisting* deformation. The reference node, through which load was applied and displacement/rotation measured, was attached through rigid elements to the top edge of the test specimen to simulate the hydraulic grips of the MTS BIONIX, see Fig. 1.

Abaqus input files are provided in the electronic annex using average thicknesses for each of the specimens, using the data presented in Table A1.

7. Results and Discussion

The *Extension-Twisting* coupling behaviour of Laminate 1 of Table 2 exists together with an inseparable *Shearing-Bending* coupling component, which is not active under tension loading. However, for the more complex coupling behaviour other Laminates 2 and 3, there is clear evidence that coupling interactions take place, and that these serves to augment the twisting response. *Bending-Twisting* coupling in Laminate 2 results in an interaction with *Shearing-Bending*, whilst the addition of *Extension-Shearing* coupling in Laminate 3 results in a further interaction between *Shearing-Bending* coupling. These responses are constrained in the experimental test and therefore lead instead to an increase in the twisting response of the specimen. At an applied load of 4.9kN, average twist angles for Laminates 1, 2 and 3 were, respectively, 9.0°, 9.5° and 12.6° from the experiments and 9.1°, 9.5° and 12.3° from the non-linear Finite element simulations. A linear analysis predicted twist angles of 10.7°, 11.1° and 14.3°, respectively. Laminate 1 provides the *Extension-Twisting* coupled baseline design test results (open circles) in Fig. 2, from which the angles correspond to a twist augmentation of 6% and 41%, for Laminate 2 (filled circles) and Laminate 3, respectively. These results can be seen to agree closely with the non-linear simulations, with twist augmentation of 4% and 36%. These twist augmentations are of course far below the 14% and 57% predictions from the constitutive equations, due to the constraining effects of the test grips and to the geometric variations in the specimens. The twist response proved to be highly sensitive to laminate thickness and in fact required careful matching of the numerical model due to the significant thickness variation between test specimens, see Table A1 of the electronic annex. Width variations also needed to be accounted for in the numerical

modelling due to inaccuracies in the waterjet cutting and some overlap in the test results is evident between Laminates 1 and 2 because of this.

Additional simulations on Laminate 3 were performed for comparison of different coupled designs with precisely matched dimensions, by directly defining the stiffness matrix terms, rather than defining a laminate stacking sequence.

Setting the *Extension-Shearing* and *Bending-Twisting* coupling terms to zero ($A_{16} = A_{26} = D_{16} = D_{26} = 0$) gave the equivalent baseline Laminate 1 result, which in this comparison produced a twist of 8.67°. Similarly, setting only the *Extension-Shearing* coupling terms to zero ($A_{16} = A_{26} = 0$, with $D_{16}, D_{26} \neq 0$) gave the equivalent baseline Laminate 2 result, with a twist of 9.30°, or an augmentation in the twist of 7.3% above the baseline. Setting only the *Bending-Twisting* coupling terms to zero ($A_{16}, A_{26} \neq 0$, with $D_{16} = D_{26} = 0$), gave rise to a new design that cannot be achieved with hygro-thermally curvature stable properties. This design resulted in a twist of 10.85°, or an augmentation in the twist of 25.1% above the baseline, demonstrating the effects of adding *Extension-Shearing* coupling only. Artificially switching the signs of A_{16} and A_{26} to those shown in Eqn. (15) reduced the twist marginally; corresponding to an augmentation of 25.0%. Finally, adding back the D_{16} and D_{26} terms from Eqn. (15) reduced the twist still further; corresponding to an augmentation of 24.8% above baseline. Reinstating the stiffnesses of Eqn. (15) gave a twist of 12.71°, or an augmentation in the twist of 46.6%, corresponding to Laminate 3.

Relaxing the effect of the grips, which was also studied only through numerical simulation, revealed that Laminate 3 does in fact exhibit secondary *Bending* and *Shearing* deflections, in addition to purely *Extension* and *Twisting* behaviour found in Laminates 1 and 2. The views of the 24mm loaded edge of the specimen in Fig. 3 highlight the (0.2mm) deformation due to tension-induced shearing and bending, when the restraining effect of the grips is removed. Whilst this more complex behaviour

could not be experimentally validated, it raises an important question about the possibility of lift augmentation in a rotating blade, as a result of complex coupling interactions.

8. Conclusion

- This study has presented an experimental study for Hygro-Thermally Curvature Stable laminate designs with precisely matched baseline stiffness properties in *Extension*, *Extension-Twisting* coupling and *Bending*, to which other a range of additional mechanical coupling behaviour have all demonstrated excellent agreement with numerical predictions, despite variations in the test specimen cross-sections.
- The addition of secondary mechanical coupling has been shown to augment substantially the *Extension-Twisting* coupling response under uniaxial axial tension. Indeed, the experimentally validated simulations have demonstrated twist augmentation above the *Extension-Twisting* coupled baseline design of approximately 12% when combined with *Bending-Twisting* coupling and approximately 47% when combined with both *Bending-Twisting* and *Extension-Shearing*.
- Numerical simulations, beyond those of the experimentally validated results, suggest that rotating blades may develop tip *bending* and *shearing* deformation, which may lead to interesting effects in the aerodynamics, including the potential for lift augmentation.

The raw data required to reproduce these findings are available to download from http://dx.doi.org/10.17632/92s86j8hny.2

Acknowledgements

The authors gratefully acknowledge Ms Zhang Linyun for assistance during the experimental testing and Mr Robert Strehle at ZwickRoell for independently verifying the experimental results.

References

1. C. B. York, A unified approach to the characterization of coupled composite laminates: Benchmark configurations and special Cases, *J. Aero. Eng., ASCE*, **23**, 2010, pp. 219-242.

2. C. B. York, Unified approach to the characterization of coupled composite laminates: Hygro-thermally curvature-stable configurations, *International Journal of Structural Integrity*, **2**, 2011, pp. 406-436.

3. C. B. York, Coupled Quasi-Homogeneous Orthotropic Laminates, *Mechanics of Composite Materials*, **47**, 2011, pp. 405-426.

4. H. P Chen, Study of hygrothermal isotropic layup and hygrothermal curvature-stable coupling composite laminates, *Proceedings of the 44th AIAA/ASME/ASCE/AHS/ASC Structures, Structural Dynamics, and Materials Conf*erence, Paper No. AIAA-2003-1506, 2003.

5. P. M. Weaver, Anisotropic Laminates that Resist Warping during Manufacture, *Proceedings of the 15th International Conference on Composite Materials*, Durban, S. Africa, 2005.

6. R. J. Cross, R. A. Haynes and E. A. Armanios. "Families of hygrothermally stable asymmetric laminated composites." Journal of Composite Materials, **42**, 2008, pp. 697-716.

7. G. Verchery, Search for Thermally Stable Laminates, *Proceedings of the 15th Composites Durability Workshop*, Kanazawa, Japan, 2010.

8. R. A. Haynes and E. A. Armanios, Hydrothermally stable laminates with extension-twist and bend-twist coupling, *Proceedings of the ICCM 18 International Conference on Composite Materials*, Jeju Island, South Korea, 2011.

9. C. B. York, Tapered hygro-thermally curvature-stable laminates with non-standard ply orientations, *Composites Part A: Applied Science and Manufacturing*, **44**, 2013, pp. 140-148.

10. ABAQUS/Standard, Version 6.14. Dassault Systèmes Simulia Corp. 2018.

Figures

Figure 1

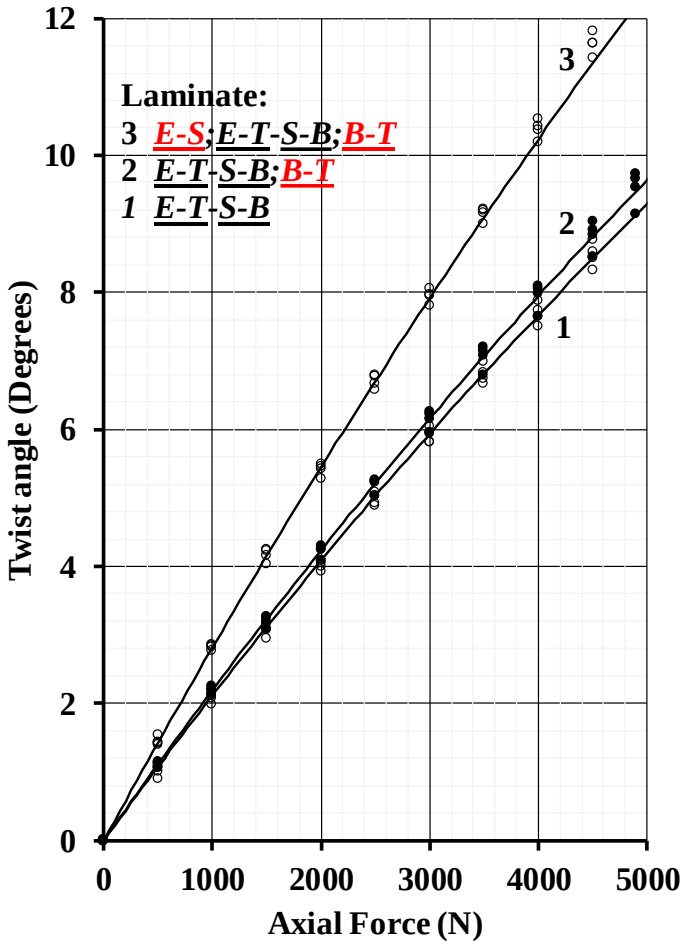
Laminate:
3 E-S;E-T-S-B;B-T
2 E-T-S-B;B-T
1 E-T-S-B
Twist angle (Degrees)
Axial Force (N)
0
2
4
6
8
10
12
0
1000
2000
3000
4000
5000
1
2
3

Figure 2

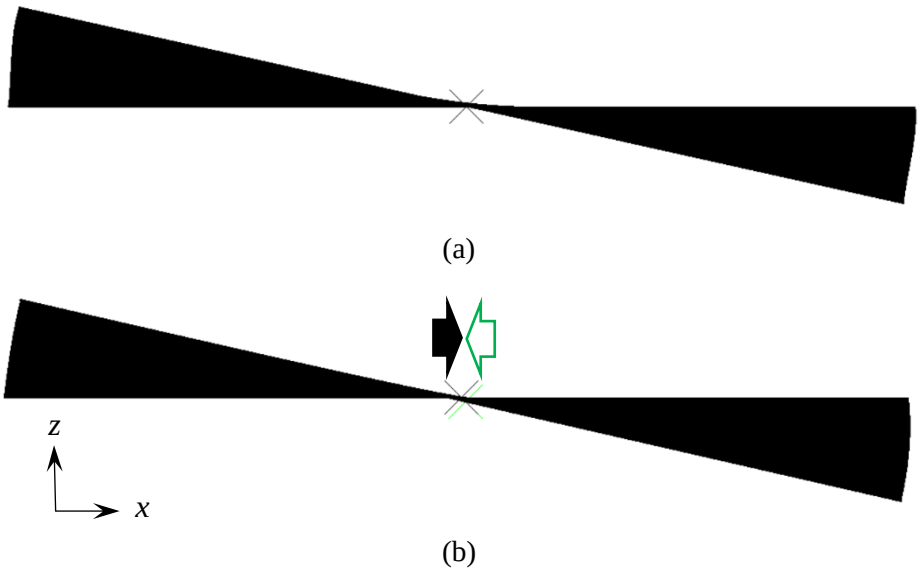

Figure 3.

Figure Captions

Figure 1. MTS BIONIX 25 kN axial-torsional machine, illustrating Laminate 1 under test (4.9 kN axial tension load, equating to Nx = 204.2 N/mm), resulting in a twist angle of 8.46°.

Figure 2. Experimental twist response of Laminates 1 – 3 of Table 2 under axial tension for laminate stacking sequences of Table 1 with $\beta = \pi/8$.

Figure 3. Numerical twist response about the loading (y-) axis for Laminate 3: (a) with and; (b) without deflection constraints applied to the loaded end to simulate the hydraulic grip movement of the experimental test.

Tables

Table 1 – Conditions for hygro-thermally curvature-stable behaviour in coupled extensionally isotropic laminates with $\xi_1 = \xi_2 = \xi_3 = \xi_4 = 0$. Lamination parameters and stiffness relationships are given with respect to material axis alignment, β.

$\beta = m\pi/2$	$\beta = \pi/8 + m\pi/2$	$\beta \neq m\pi/2,\ \pi/8 + m\pi/2$
(m = 0, 1, 2, 3)	(m = 0, 1, 2, 3)	(m = 0, 1, 2, 3)
E-B-*S-T*	*E-T*-*S-B*	*E-B*-*S-B*-*E-T*-*S-T*
$\begin{bmatrix} B_{11} & -B_{11} & 0 \\ -B_{11} & B_{11} & 0 \\ 0 & 0 & -B_{11} \end{bmatrix}$	$\begin{bmatrix} 0 & 0 & B_{16} \\ 0 & 0 & -B_{16} \\ B_{16} & -B_{16} & 0 \end{bmatrix}$	$\begin{bmatrix} B_{11} & -B_{11} & B_{16} \\ -B_{11} & B_{11} & -B_{16} \\ B_{16} & -B_{16} & -B_{11} \end{bmatrix}$
$\xi_5 = \xi_7 = \xi_8 = 0$	$\xi_5 = \xi_6 = \xi_7 = 0$	$\xi_5 = \xi_7 = 0$

Table 2 – Laminate designs and mechanical properties, as manufactured, $\beta = 0°$, and as tested, $\beta = \pi/8$.

Ref.	Stacking Sequence, $\beta = 0°$	Coupling, $\beta = 0°$ ($\pi/2$)	Coupling, $\beta = \pi/8°$ ($+ \pi/2$)	Stacking Sequence, $\beta = \pi/8°$
1	$[-45_2/45_2/0/45/-45/90/45/0/90/-45/90_2/0_2]_T$	*E-B*-*S-T*;*B-T*	*E-T*-*S-B*	$[-22.5_2/67.5_2/22.5/67.5/-22.5/-67.5/67.5/22.5/-67.5/-22.5/-67.5_2/22.5_2]_T$
2	$[-45/0/45_3/-45_3/90/45/90_2/0/90/0_2]_T$	*E-B*-*S-T*	*E-T*-*S-B*;*B-T*	$[-22.5/22.5/67.5_3/-22.5_3/-67.5/67.5/-67.5_2/22.5/-67.5/22.5_2]_T$
3	$[-45/45_2/-45/0_3/90_6/0_3]_T$	*E-B*-*S-T*	*E-S*;*E-T*-*S-B*;*B-T*	$[-22.5/67.5_2/-22.5/22.5_3/-67.5_6/22.5_3]_T$

Electronic Annex to: Test Validation of Extension-Twisting coupled Laminates with Matched Orthotropic Stiffness.

Table A1: Geometry for each of the four samples, corresponding to the three laminate designs of Table 2.

(a) – Laminate 1

		Specimen thickness				Specimen width			
Position:	Top	2.43	2.62	2.59	2.58	24.05	24.09	24.08	24.05
	Middle	2.56	2.62	2.63	2.63	24.07	24.06	24.15	24.16
	Bottom	2.60	2.66	2.70	2.64	24.02	24.09	24.12	24.10
Laminate:	Average *H*	2.53	2.63	2.64	2.62	24.05	24.08	24.11667	24.10
Ply:	Average *t*	0.158	0.165	0.165	0.164				

(b) – Laminate 2

		Specimen thickness				Specimen thickness			
Position:	Top	2.53	2.57	2.62	2.66	24.05	24.09	24.08	24.05
	Middle	2.61	2.65	2.69	2.66	24.07	24.06	24.15	24.16
	Bottom	2.61	2.67	2.70	2.70	24.02	24.09	24.12	24.10
Laminate:	Average *H*	2.58	2.63	2.67	2.67	24.05	24.08	24.12	24.10
Ply:	Average *t*	0.161	0.164	0.167	0.167				

(c) – Laminate 3

		Specimen thickness				Specimen thickness			
Position:	Top	2.61	2.69	2.64	2.7	23.64	23.8	23.86	23.57
	Middle	2.64	2.66	2.63	2.67	23.57	23.83	23.59	23.49
	Bottom	2.66	2.66	2.62	2.68	23.67	23.82	23.74	23.64
Laminate:	Average *H*	2.64	2.67	2.63	2.68	23.63	23.82	23.73	23.57
Ply:	Average *t*	0.165	0.167	0.164	0.168				

Figure A1 – Gauge length measurement confirmed from indentations on test specimens from bevel edged serrated grips.

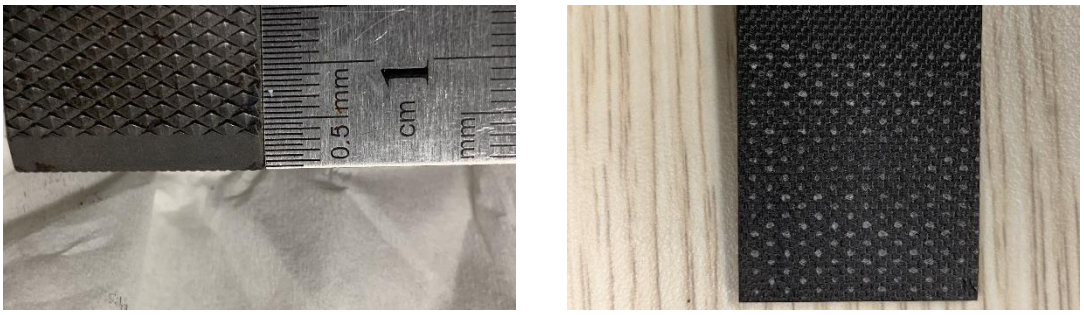

ABAQUS Input Files:

LAMINATE 1

```
*HEADING
EXTENSION-TWISTING TEST SPECIMEN
*NODE
1001,0,0,0
1025,24.07,0,0
201001,0,189,0
201025,24.07,189,0
300000,12,199,0
*NSET,NSET=RNODE
300000
*NGEN,NSET=TOP
201001,201025
*NGEN,NSET=BOTTOM
1001,1025
*NFILL,NSET=ALL
BOTTOM,TOP,200,1000
*ELEMENT,TYPE=S4R
1001,1001,1002,2002,2001
*ELGEN,ELSET=PLATE
1001,24,1,1,200,1000,1000
*RIGID BODY, REF=RNODE,TIENSET=TOP
*MATERIAL,NAME=CFRP
*ELASTIC,TYPE=LAMINA
131E3,8.2E3,0.38,4.3E3,4.3E3,2.2E3
*SHELL SECTION,ELSET=PLATE,COMPOSITE
**Laminate 1
0.152,3,CFRP,-22.5,PLY_1
0.152,3,CFRP,-22.5,PLY_2
0.152,3,CFRP,67.5,PLY_3
0.152,3,CFRP,67.5,PLY_4
0.152,3,CFRP,22.5,PLY_5
0.152,3,CFRP,67.5,PLY_6
0.152,3,CFRP,-22.5,PLY_7
0.152,3,CFRP,-67.5,PLY_8
0.152,3,CFRP,67.5,PLY_9
0.152,3,CFRP,22.5,PLY_10
0.152,3,CFRP,-67.5,PLY_11
0.152,3,CFRP,-22.5,PLY_12
0.152,3,CFRP,-67.5,PLY_13
0.152,3,CFRP,-67.5,PLY_14
0.152,3,CFRP,22.5,PLY_15
0.152,3,CFRP,22.5,PLY_16
*BOUNDARY
BOTTOM,ENCASTRE
```

```
RNODE,1
RNODE,3,4
RNODE,6
*STEP, INC=7500, NLGEOM
*STATIC,RIKS
0.01, 1., 1.E-5, 0.01, 1
*CLOAD
RNODE,2,5000
*RESTART,WRITE,FREQUENCY=0
*OUTPUT,FIELD,VARIABLE=PRESELECT
*OUTPUT,HISTORY
*NODE OUTPUT,NSET=RNODE
CF2,UR2
*END STEP
```

LAMINATE 2

Change only the nodal data and laminate description from the above input file, as follows:

```
*NODE
1001,0,0,0
1025,24.11,0,0
201001,0,189,0
201025,24,189,0
300000,12,199,0

**Laminate 2
0.159,3,CFRP,-22.5,PLY_1
0.159,3,CFRP,22.5,PLY_2
0.159,3,CFRP,67.5,PLY_3
0.159,3,CFRP,67.5,PLY_4
0.159,3,CFRP,67.5,PLY_5
0.159,3,CFRP,-22.5,PLY_6
0.159,3,CFRP,-22.5,PLY_7
0.159,3,CFRP,-22.5,PLY_8
0.159,3,CFRP,-67.5,PLY_9
0.159,3,CFRP,67.5,PLY_10
0.159,3,CFRP,-67.5,PLY_11
0.159,3,CFRP,-67.5,PLY_12
0.159,3,CFRP,22.5,PLY_13
0.159,3,CFRP,-67.5,PLY_14
0.159,3,CFRP,22.5,PLY_15
0.159,3,CFRP,22.5,PLY_16
```

LAMINATE 3:

Change only the nodal data and laminate description from the above input file, as follows:

```
*NODE
1001,0,0,0
1025,23.72,0,0
201001,0,189,0
201025,23.69,189,0
300000,12,189,0

**Laminate 3
0.163,3,CFRP,-22.5,PLY_1
0.163,3,CFRP,67.5,PLY_2
0.163,3,CFRP,67.5,PLY_3
0.163,3,CFRP,-22.5,PLY_4
0.163,3,CFRP,22.5,PLY_5
0.163,3,CFRP,22.5,PLY_6
0.163,3,CFRP,22.5,PLY_7
0.163,3,CFRP,-67.5,PLY_8
0.163,3,CFRP,-67.5,PLY_9
0.163,3,CFRP,-67.5,PLY_10
0.163,3,CFRP,-67.5,PLY_11
0.163,3,CFRP,-67.5,PLY_12
0.163,3,CFRP,-67.5,PLY_13
0.163,3,CFRP,22.5,PLY_14
0.163,3,CFRP,22.5,PLY_15
0.163,3,CFRP,22.5,PLY_16
```